

Potential formalism for an axial energy cumulation process

Shalom Eliezer* and José M. Martínez-Val

Escuela Técnica Superior de Ingenieros Industriales, José Gutiérrez Abascal 2, 28006 Madrid, Spain

(Received 2 November 1998; revised manuscript received 26 June 2000)

A central filament is assumed to be axially positioned inside a collapsing cylindrical thin shell. A cumulation process is induced by generating a high magnetic field between the shell and the filament. Assuming a dissipationless approach, it is shown that this problem is equivalent to two point particles moving in a potential.

PACS number(s): 52.55.-s, 52.75.-d

Cumulation, i.e., concentration of energy (or magnetic fields or any other physical quantity) into a small volume is well under research and development in pulse power devices. In particular, different imploding Z-pinch devices have been investigated [1–4]. The concentration of energy into a small fiber plasma provides extremely high temperatures, which might pave the way to thermonuclear fusion and other technical applications.

Two scenarios can be considered for the model described in this paper, where a central filament is assumed to be axially positioned inside a cylindrical shell collapsing by the Z-pinch effect. The cumulation process is induced by generating a high magnetic field between the cylindrical shell and the filament.

(a) The first scenario presumes that the central filament is a porous material with a density of the order of the plasma critical density (i.e., the number of electrons per cm^3 is $10^{21}/\lambda_\mu^2$, where λ_μ is the laser wavelength in μm). Circularly polarized laser light (CPLL) is absorbed along the filament and by the inverse Faraday effect induces an axial magnetic field between the filament and the shell. Recently, megagauss axial magnetic fields have been measured [5,6] in laser plasma interactions.

In the CPLL scenario, another configuration can be taken into account: the filament is solid (with a density larger than the critical density) and a porous material is placed between the filament and the shell. The laser light is absorbed between the shell and the filament and a reversed field configuration is generated (between the filament and the shell). In this case the magnetic field inside the filament is zero, assuming a dissipationless system.

(b) An external magnetic field B_{z0} is applied between the shell and the filament. In this case the field coils are outside the shell, and an ideal dissipationless system must be assumed, so that the magnetic field does not penetrate into the filament (i.e., it behaves as a superconducting plasma).

The two scenarios (a) and (b) are not equivalent. CPLL induced magnetic fields require a technique still under development, with very promising results [5,6]. It could actually produce powerful magnetic fields on a very short time scale, of the order of 100 ps or less. In contrast, external coils are more conventional, but they need a much longer time to be created, which also means they have more time for diffusing

into the surrounding plasmas. Here we propose to use the inverse Faraday effect by propagating circularly polarized laser light along an underdense layer of the filament (a coating). Therefore we shall analyze case (a) in particular.

The filament length over which the inverse Faraday effect is effective can be estimated by assuming that the laser absorption is due to inverse bremsstrahlung. In this case the length l in units of cm is inversely proportional to the absorption coefficient.

$$l \approx 3.4(T_e^{1.5})\lambda_L^{-2}(10^{20}/n_e)^2(1/Z),$$

where T_e and n_e are the electron temperature (in keV) and density (in units of cm^{-3}), Z is the plasma ionization, and λ_L is the laser wavelength (in μm). For $\lambda_L \approx 1 \mu\text{m}$, $n_e \approx \frac{1}{3} \times 10^{21} \text{cm}^{-3}$ ($\frac{1}{3}$ the critical density), $T_e = 1 \text{keV}$, and $Z = 1$, one gets $l \approx 0.15 \text{cm}$.

Besides the axial magnetic field B_z created by the inverse Faraday effect, there is also an azimuthal magnetic field B_θ generated by a term of the form $\partial B_\theta / \partial t = \nabla n_e \times \nabla [T_e / (en_e)]$ which implies that $B_\theta \approx T_e \tau_l / (L_n L_T)$, where L_n is a scale length in the axial direction and in our case is of the order of the filament length and L_T is a transverse scale length and in our case is of the order of the filament radius. With $L_n \approx 0.1 \text{cm}$, $T_e \approx 1000 \text{eV}$, $L_T \approx 0.005 \text{cm}$, and a laser pulse duration of the order of 1 ns, we can expect that $B_\theta / B_z \ll 10^{-3}$, so that the interchange instability modes are not important.

Another issue is the Rayleigh-Taylor (RT) instabilities. There are two phases where they can destroy the cylindrical symmetry: (1) the Z pinch of the shell during its acceleration phase and (2) the filament acceleration by the magnetic field between the cylindrical shell and the filament. The first one is typical of any Z-pinch scheme and this instability may be reduced by the scheme where multiwire shells are imploded [8–10]. The second one is typical of our scheme and it is analyzed following Chandrasekhar [11]. The amplitude of the RT instability is proportional to $\exp(\Gamma t)$; the growth rate Γ is given by

$$\Gamma^2 = gk \left(\frac{\rho_2 - \rho_1}{\rho_2 + \rho_1} - \gamma \right), \quad (1)$$

where g is the acceleration, ρ_2 and ρ_1 are the densities of the heavy and light fluids (the magnetic field acts as the lightest

*On leave from SOREQ NRC, Yavne 81800, Israel.

fluid with zero density), $k=2\pi/\lambda$ where λ is the wavelength of the instability, and $\gamma=B_z^2/2g\rho\lambda$.

As $\rho_1=0$, when $\gamma\geq 1$ the implosion is stabilized by the applied magnetic field. It must be noted that γ depends on λ and it is easier to stabilize short-wavelength modes than long-wavelength perturbations. Of course, wavelengths cannot very long because they are approximately limited to the shell diameter. For instance, for $B_{z0}=4$ MG and a relevant acceleration of 10^{15} cm/s² during the interaction phase between the shell and the filament, one obtains $\gamma\lambda\sim 0.5$. Therefore, for this example, the axial magnetic field reduces instabilities due to perturbations with amplitude smaller than about 0.5 cm.

The current generated by the CPLL will also produce a magnetic field inside the hollow filament in the opposite direction to that between the shell and the filament, so that the net flux is zero. For a filament of radius a and a shell of radius r , flux conservation requires

$$B_z(\text{in})a^2=B_z(\text{out})(r^2-a^2), \quad (2)$$

where ‘‘in’’ and ‘‘out’’ refer to inside and outside the filament.

In our model, the analysis will be restricted to the ‘‘collision’’ between the shell and the filament, i.e., the interaction phase where the shell approaches the filament, and therefore $(r-a)\ll a$, and $B_z(\text{in})\ll B_z(\text{out})$. The magnetic field must be switched off once the bulk of the filament has already been accelerated toward the axis. From that point on, the implosion is driven only by the kinetic energy transmitted from the shell to the filament and it becomes a standard problem of inertial confinement. The CPLL is applied only in that period of time, which means that a short-pulse laser triggered around the collision time is the suitable tool for this purpose.

Using this ‘‘CPLL scenario,’’ the laser duration time scale is much less than the time scale of the magnetic diffusion (into the filament). In fact, a characteristic magnetic diffusion time would be

$$\tau_B=\frac{4\pi\sigma l^2}{c^2}, \quad (3)$$

where l is the diffusion penetration length, c is the speed of light, and σ is Spitzer’s conductivity [7] in units of s⁻¹ given by

$$\sigma=\frac{8.70\times 10^{13}}{Z\ln\Lambda}T_e^{3/2} \quad (4)$$

with T_e in eV. Therefore, for a Coulomb logarithm $\ln\Lambda\sim 10$, we have

$$\tau_B=3.84\times 10^{-5}\left(\frac{1}{Z}\right)T_e^{3/2}l^2, \quad (5)$$

where τ_B is given in s, T_e in keV, and l in mm. For length dimensions smaller than the filament radius, e.g., $10\ \mu\text{m}$, and a temperature of 1 keV, the diffusion time becomes $\tau_B\approx 4$ ns. Although this estimate is relevant for the initial stages of the magnetic penetration (in planar geometry), the diffusion time in a cylindrical geometry is reduced by a fac-

tor equal to the square of the first root of the Bessel function of order 1. In the above example the diffusion time is reduced to 0.3 ns.

The equation of motion for a thin shell of matter, assuming axial symmetry, is given in cylindrical coordinates by

$$\rho_s\frac{d^2r}{dt^2}=-\frac{\partial P_s}{\partial r}, \quad r_1(t)\leq r\leq r_2(t), \quad (6)$$

where ρ_s and P_s are the shell density and pressure, respectively. In order to write the equation of motion for an average radial distance $\langle r \rangle$ we define

$$\langle f(r) \rangle = \frac{2\int_{r_1}^{r_2} f(r)r\,dr}{(r_2^2-r_1^2)}. \quad (7)$$

Using the approximation $r_2^2-r_1^2=2\langle r \rangle d$, where $d=r_2-r_1$ and $\langle r \rangle\approx r_1\approx r_2$, and introducing the shell mass per unit length $M_s=\rho_s 2\pi\langle r \rangle d$ into Eq. (6), one gets

$$M_s\frac{d^2\langle r \rangle}{dt^2}=-2\pi\int_{r_1}^{r_2} r\frac{\partial P_s}{\partial r}dr=-2\pi[r_2P_s(r_2)-r_1P_s(r_1)], \quad (8)$$

where the right-hand side was obtained by integrating by parts and assuming the thin shell approximation

$$\int_{r_1}^{r_2} P_s dr\ll P(r)r \quad \text{for } r_1\leq r\leq r_2. \quad (9)$$

Through the shell, a current I_s flows in the axial direction and the shell implodes onto the coaxial target (the filament). This current creates an outer toroidal magnetic field B_θ , implying a pressure $P_s(r_2)$ of

$$P_s(r_2)=\frac{B_\theta^2}{8\pi}, \quad (10)$$

$$B_\theta=\frac{I_s}{5r_2}. \quad (11)$$

In these equations, cgs units are used, except for the current which is in ampères.

I_s is the value of the maximum current. The current in a Z-pinch discharge is time dependent with a time scale variation of the order of $1\ \mu\text{s}$. However, the time scale of the process considered in this paper is of the order of 1 ns. Therefore one may assume that the current I_s is constant for the calculations presented here.

An axial magnetic field B_{z0} is created as described above in scenario (a) or (b). The magnetic field B_z between the shell and the filament and its pressure are obtained by using the flux conservation principle,

$$B_{z0}(r_0^2-a_0^2)=B_z(r^2-a^2), \quad (12)$$

$$P_m(r)=\frac{B_z^2}{8\pi}, \quad (13)$$

where r_0 and a_0 are the radius of the shell [$r_0=r(t=0)$] and the filament [$a_0=a(t=0)$] at the time when the magnetic

field is created. Substituting $P_s(r_2)$ from Eq. (10) and $P_s(r_1)$ from Eq. (13) into Eq. (8), one gets the equation of motion of the shell for a thin shell approximation ($\langle r \rangle = r \approx r_1 \approx r_2$),

$$M_s \frac{d^2 r}{dt^2} = -\frac{I_s^2}{100r} + \frac{B_{z0}^2 r}{4} \left(\frac{r_0^2 - a_0^2}{r^2 - a^2} \right)^2. \quad (14)$$

The equation of motion for the target, i.e., the central filament, is given by

$$\rho_f \left(\frac{\partial u}{\partial t} + u \frac{\partial u}{\partial r} \right) = -\frac{\partial P_f}{\partial r}, \quad (15)$$

where u , ρ_f , and P_f are the filament speed, density, and pressure, respectively.

Uniform pressure and velocity profiles are assumed inside the filament. When the magnetic pressure between the shell and the filament, P_m , is larger than the filament pressure P_f , the implosion process takes place with a negative velocity u . Similarly, for $P_f > P_m$ the filament expands with a positive velocity. The pressure can be written as $P = P_f \theta(a-r) + P_m \theta(r-a)$, where $\theta(x) = 1$ for $x > 0$ and $\theta(x) = 0$ for $x < 0$. Similarly, the velocity $u(r, t) = u_0(t) \theta(a-r) = (da/dt) \theta(a-r)$. Therefore the equation of motion of the filament is

$$\rho_f \frac{d^2 a}{dt^2} = -\frac{P_f - P_m}{a}. \quad (16)$$

The filament is assumed to be in a plasma state with a pressure composed of two terms, P_T , the ideal gas equation of state (EOS), and P_c , taken as the Fermi-Dirac pressure [12] (the cold EOS),

$$P_f = P_c + P_T, \quad (17)$$

$$P_T = (1+Z)n_i k_B T, \quad (18)$$

$$P_c = \frac{1}{20} \left(\frac{3}{\pi} \right)^{2/3} \frac{h^2}{m_e} n_e^{5/3} \equiv c_e n_e^{5/3}. \quad (19)$$

n_e and n_i are the electron and ion number densities of the filament plasma, which is assumed to be neutral; $n_e = Zn_i$, Z being the average degree of ionization. The electrons and the ions are assumed to have the same temperature $T_e = T_i = T$. In Eq. (18) k_B is the Boltzmann constant, h is the Planck constant, and m_e is the electron mass. Introducing into Eq. (19) the filament mass per unit length $M_f = \pi a^2 \rho_f$, and using the relation $n_i = \rho_f / (A_f m_p)$, where m_p is the proton mass and A_f is the atomic number of the filament matter, the filament pressure is expressed by

$$P_f = (1+Z) \left(\frac{M_f}{A_f m_p} \right) \frac{k_B T}{\pi a^2} + \left(\frac{Z}{\pi} \right)^{5/3} \left(\frac{M_f}{A_f m_p} \right)^{5/3} \frac{c_e}{a^{10/3}}. \quad (20)$$

Note that $P_c(\rho_0)/P_T(10 \text{ eV}) \sim 0.2$ where ρ_0 is the DT liquid density, and this ratio scales with density and temperature as $\rho_f^{2/3}/T$.

Assuming an adiabatic energy equation for the filament, $T/\rho_f^{2/3} = \text{const}$, one has

$$\left(\frac{T}{T_0} \right) = \left(\frac{a_0}{a} \right)^{4/3}. \quad (21)$$

Using Eqs. (20) and (21) in Eq. (17), the equation of motion (16) of the filament is derived:

$$M_f \frac{d^2 a}{dt^2} = \left[2(1+Z)k_B T_0 a_0^{4/3} \left(\frac{M_f}{A_f m_p} \right) + \frac{10c_e Z^{5/3}}{3\pi^{2/3}} \left(\frac{M_f}{A_f m_p} \right)^{5/3} \right] \frac{1}{a^{7/3}} - \frac{B_{z0}^2 a}{4} \left[\frac{r_0^2 - a_0^2}{r^2 - a^2} \right]^2. \quad (22)$$

The equations of motion of shell and filament, Eqs. (14) and (22), can be derived from a potential $U(r, a)$ given by (in cgs units but I_s in A)

$$U(r, a) = A \ln \frac{r}{r_0} + \frac{B}{2} \left(\frac{a^2 - a_0^2}{r^2 - a^2} - \frac{r^2 - r_0^2}{r^2 - a^2} \right) + C \left[\left(\frac{a_0}{a} \right)^{4/3} - 1 \right], \quad (23)$$

$$A = \frac{I_s^2}{100}, \quad B = \frac{1}{4} B_{z0}^2 (r_0^2 - a_0^2), \quad C = C_c + C_T, \quad (24)$$

$$C_c = (1.45 \times 10^{13}) \left(\frac{Z M_f}{A_f} \right)^{5/3} \frac{1}{a_0^{4/3}}, \quad C_T = 2(1+Z)k_B T_0 \left(\frac{M_f}{A_f m_p} \right). \quad (25)$$

Note that A, B, C are positive and have dimensions of erg/cm.

A classical Hamiltonian H can be defined for the canonical variables r and p_s and a and p_f

$$p_s = M_s \frac{dr}{dt}, \quad (26)$$

$$p_f = M_f \frac{da}{dt}, \quad (27)$$

$$H = \frac{p_s^2}{2M_s} + \frac{p_f^2}{2M_f} + U(r, a), \quad (28)$$

with the usual equations of motion

$$M_s \frac{d^2 r}{dt^2} = -\frac{\partial U}{\partial r}, \quad (29)$$

$$M_f \frac{d^2 a}{dt^2} = -\frac{\partial U}{\partial a}, \quad (30)$$

which correspond to the Hamilton-Jacobi equations. Equations (29) and (30) are identical to Eqs. (14) and (22). In this formalism the magnetic field B_{z0} and the current I_s are constants. The ‘‘potential’’ formalism is applicable only after the B_{z0} is induced (by the action of the CPL beam or by external coils). Before it, the shell is strongly accelerated inward by the pinch effect.

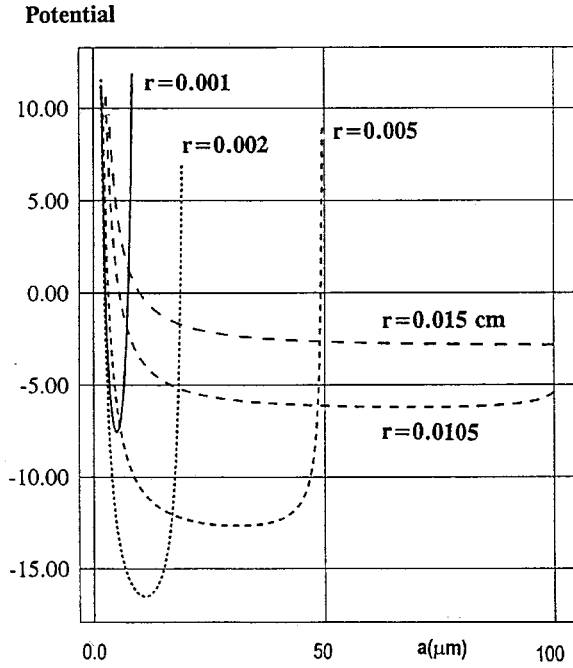


FIG. 1. The potential $U(r, a)$ as a function of the filament radius a with the thin shell position r as a parameter (potential unit=100 J). Shell mass is $46.4 \mu\text{g/cm}$; filament mass $11.6 \mu\text{g/cm}$; maximum pinch current 1 MA; axial magnetic field 10^6 G ; initial shell radius 0.02 cm; initial filament radius 0.01 cm; initial filament temperature due to laser interaction 10 eV. The filament is made of deuterium. It is important to observe that the potential shows a significant well as the radius r decreases.

The extremum of the potential is given by solving $\partial U/\partial r=0$, $\partial U/\partial a=0$, implying that

$$\frac{A}{B(r_0^2 - a_0^2)} = \frac{r^2}{(r^2 - a^2)^2}, \quad (31)$$

$$\frac{4Ca_0^{4/3}}{3B(r_0^2 - a_0^2)} = \frac{a^{10/3}}{(r^2 - a^2)^2}. \quad (32)$$

For $Z=1$, the solution of these equations is given in practical units by

$$\frac{r}{r_0} = \frac{0.132}{A_f^{1/6}} r_0^{14/9} a_0^{2/9} T_0^{1/6} M_f^{1/6} B_{z0}^{7/9} I_s^{-10/9}, \quad (33)$$

$$\frac{a}{a_0} = \frac{(9.39 \times 10^{-2})}{\sqrt{A_f}} r_0^{2/3} a_0^{2/3} T_0^{1/2} M_f^{1/2} B_{z0}^{1/3} I_s^{-4/3}, \quad (34)$$

with r_0 in mm, a_0 in units of 0.1 mm, T_0 in eV, M_f in $\mu\text{g/cm}$, B_{z0} in MG and I_s in MA.

An analysis of the potential U as a function of a for r as a parameter is given in Fig. 1. From the numerical solutions in Fig. 1 it is clear that interaction between the two masses is analogous to an elastic collision of point particles with a reflecting wall at $a=0$.

The efficiency of the filament implosion depends on the hydrodynamic efficiency of the shell-filament collision, i.e.,

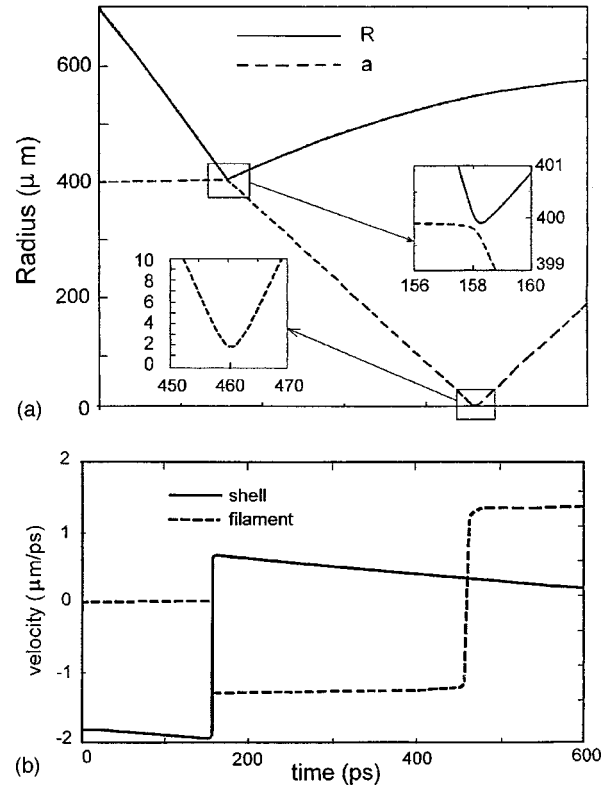


FIG. 2. (a). Numerical calculations for the filament (a) and shell (r) positions as a function of time, for $I_s=25 \text{ MA}$, $B_{z0}=4 \text{ MG}$, $T_0=10 \text{ eV}$, and $M_s=M_f$ with initial shell speed of $1.8 \mu\text{m/ps}$. (b) Evolution of the shell and filament speeds in the case presented in (a).

on the fraction of the kinetic energy of the shell transmitted to the filament. If a head-on elastic collision is assumed, it can be estimated by

$$\frac{V_f}{V_s} = \frac{2(M_s/M_f)}{(M_s/M_f) + 1}, \quad (35)$$

and

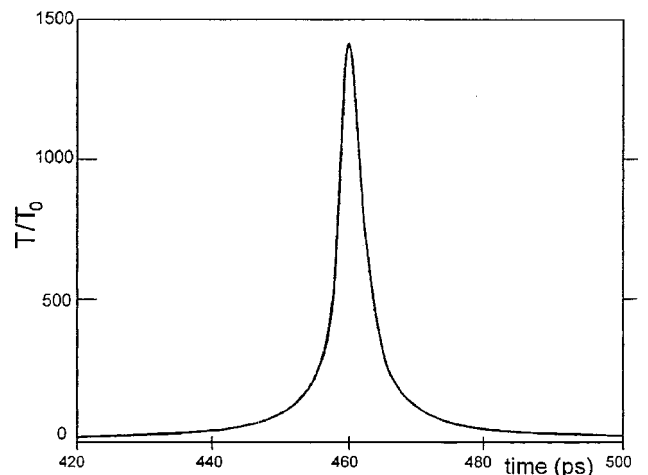


FIG. 3. Filament temperature vs time for the case reported in Fig. 2.

$$\eta = \frac{M_f V_f^2}{M_s V_s^2} = \frac{4(M_s/M_f)}{(M_s/M_f)^2 + 2(M_s/M_f) + 1}, \quad (36)$$

where V_f and V_s are the velocity of the filament and the shell, respectively. η gets its maximal value ($\eta=1$) for $M_s/M_f=1$, which corresponds to the classical billiard head-on collision, in which the incoming ball is stopped and the ball at rest goes out with the speed of the former. In inertial confinement fusion (ICF) the speed of the imploding matter is very important. From Eq. (35) one can see that V_f/V_s increases as M_s/M_f increases, with the asymptotic value of 2. However, in our model the shell mass is limited by the thin shell approximation.

In Figs. 2(a) and (2b) the shell and filament positions and their appropriate velocities are given for $\eta=1$ (i.e., $M_s = M_f$). Values assumed for the electromagnetic parameters are very high, as needed for fusion scenarios, namely, $B_{z0} = 4$ MG, $I_s = 25$ MA, and a deuterium-tritium target with ini-

tial temperature $T_0 = 10$ eV. In these numerical calculations, B_z is switched off after the shell-filament ‘‘collision.’’ The temperature of the filament for this case is given in Fig. 3. Values over 10 keV are obtained inside the filament around the time of maximum compression. This temperature would be high enough to trigger a DT fusion burst, which is a positive conclusion of our analysis. However, additional analysis of density values and confinement time is needed to have a complete picture of the importance of this scheme for future fusion applications. In any case, the potential formalism is a kinematic view of the cumulation process that could be created in the interaction between coaxial plasmas separated by a magnetic field.

We would like to extend our thanks to Z. Henis and I. Vorobeichik for useful discussions, and to I. Vorobeichik also for his valuable numerical calculations. This work was supported in part by Spain’s Ministry of Education, Science and Culture.

-
- [1] *Megagauss Technology and Pulsed Power Applications*, edited by C. M. Foulter, R. S. Caird, and D. J. Eriksion (Plenum New York, 1987).
- [2] H. U. Rahman, F. J. Wessel, and N. Rostoker, *Phys. Rev. Lett.* **74**, 714 (1995).
- [3] V. Simrnov *et al.*, in *Dense Z-Pinches*, edited by M. Haines and A. Knight, AIP Conf. Proc. No. 299 (AIP, New York, 1994).
- [4] M. A. Liberman, J. S. DeGroot, A. Toor, and R. B. Spileman, *Physics of High Density Z-Pinch Plasmas* (Springer, New York, 1999).
- [5] Y. Horovitz *et al.*, *Phys. Rev. Lett.* **78**, 1707 (1997).
- [6] Y. Horovitz *et al.*, *Phys. Lett. A* **245**, 329 (1998).
- [7] L. Spitzer, Jr., *Physics of Fully Ionized Gases* (Wiley Interscience, New York, 1962).
- [8] M. K. Matzen, *Phys. Plasmas* **4**, 1519 (1997).
- [9] R. B. Spielman *et al.*, *Phys. Plasmas* **5**, 2105 (1998).
- [10] C. Deeney *et al.*, *Phys. Rev. Lett.* **81**, 4883 (1998).
- [11] S. Chandrasekhar, *Hydrodynamic and Hydromagnetic Stability* (Dover, New York, 1961), p. 466.
- [12] S. Eliezer, A. K. Ghatak, and H. Hora, *An Introduction to Equations of State, Theory and Applications* (Cambridge University Press, Cambridge, U.K., 1986).